

Modelling and Accident Reconstruction of Head Impact Injuries

Michael D. Gilchrist

Department of Mechanical Engineering, University College Dublin, Belfield, Dublin 4, Ireland,
Michael.Gilchrist@ucd.ie

Keywords: Head injury; neurotrauma; impact; accident reconstruction

Abstract. This paper describes a computational mechanics framework within which the physiological consequences of an accidental head impact injury can be simulated. This method relies on a combined use of multibody dynamics and finite element analyses. Such a procedure could ultimately be used to assist in the clinical diagnosis of neurotrauma and in the design of optimised safety helmets.

Introduction

Mechanical impact is the leading cause of injury, death and disability in people aged under 45 in the USA, Europe and increasingly so in Third World countries [1]. Head impact injuries account for approximately half of all deaths due to mechanical trauma, but account for the majority of cases of disability after injury. Despite increased use of protective devices such as seat belts, airbags, safety restraints and safety helmets, brain injury disables or kills someone in the United States every two and a half minutes. In addition to the huge human cost to society, the financial cost of hospitalisation, care and rehabilitation of head injured people has been estimated to be as high as \$33 billion per year in the US alone [2].

Road traffic accidents (RTAs), falls and assaults are the most frequently cited causes of head injury. However, the ratios of these three differ worldwide, as summarised in Fig. 1. While RTAs tend to be the leading cause of injury related death, falls tend to be the leading cause of non-fatal hospitalisation [6, 7]. In Ireland, falls are the single greatest cause of hospital admissions for both males and females across most age groups, with head injuries occurring in approximately a quarter of fall admissions [7]. It is also important to note that RTAs and falls generally lead to different types of trauma. While RTAs tend to cause diffuse and multifocal injuries, the type of head injuries received from falls tend to be focal. Contrecoup injury, where the injury occurs at the contralateral side to the site of impact, is particularly prevalent with falls, while ipsilateral (or coup) injury rarely occurs except in cases involving skull fracture [8, 9].

Due to its complex nature, functional and traumatic injuries to the brain are difficult to quantify and it is because of this complexity that a variety of alternative mechanisms have been proposed for explaining the development of brain injury. All theories, however, agree that injury is related to acceleration or deceleration of the head regardless of whether the impact is applied directly or indirectly. The brain is loosely coupled to the skull and consequently its motion will lag that of the skull, resulting in 'bruising' of the brain as it impacts against the interior surface of the skull. Stretching of the tethering blood vessels, which arises as a result of this lag in motion, can cause them to strain excessively, rupture, fail and bleed. The brain tissue itself may be damaged by normal and shear forces that develop during translational and rotational accelerations or decelerations.

Biomechanical research attempts to understand the development of injury and thereby help to avoid or alleviate the damage that can occur from various impacts. This can only be achieved by first understanding the mechanics of impact and the biomechanical response of the head (i.e., the skull-brain system) to a variety of loading conditions. Brain injury mechanisms are generally

described in terms of the mechanical and physiological changes that result in anatomical and functional damage [10].

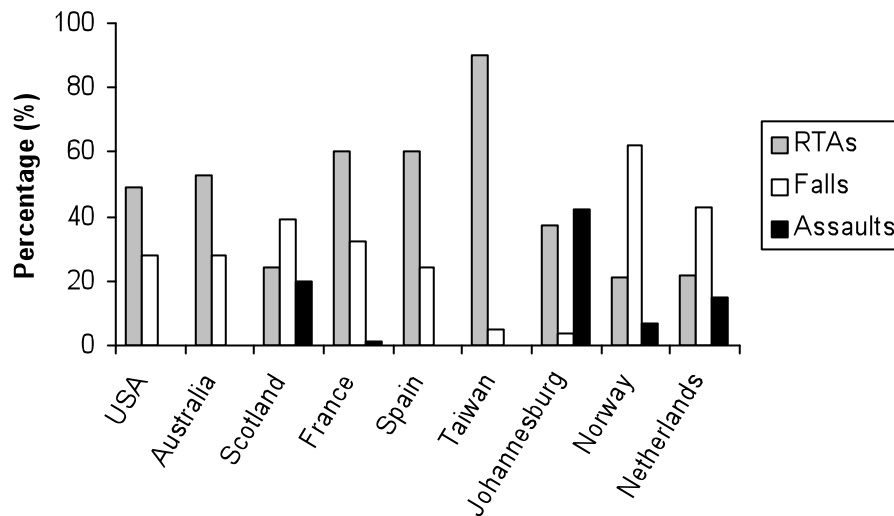


Figure 1. Distribution of causes of head injury worldwide [1,3-5].
Where no column is represented, there is no information for that statistic.

The constitutive properties of both the skull and brain influence the system response to mechanical loads and must be known if the physical response of the skull-brain system is to be predicted accurately [11]. This has posed significant difficulties for researchers in recent decades following the development of more powerful computational resources [12], since the properties of living human tissue deviate from those of cadavers and primates and no harmless non-invasive procedures for establishing such properties in vivo have been established.

Physiology of the Human Head

The skull has often been modelled as a sphere, but in reality it is closer to an ellipsoid that is narrower towards the front of the head. It has been suggested by many [13-15] and confirmed analytically [16] and computationally [17] that this eccentricity will influence the response of the head to an impact. The frontal bone provides greater resistance to stress due to its curvature. If the skull were represented by a discrete distribution of sprung masses, the stiffness of the skull would be different for each impact scenario because the structural response is dependent on all of the springs involved. In addition, the radius of curvature of the skull is different throughout: in some areas it is much more rounded while in others it is much flatter.

The cerebrospinal fluid (CSF) acts as an important energy damping mechanism during impact of the skull brain system [18-20]. Higher contrecoup injuries have been witnessed when high accelerations before impact are involved, such as develop in a fall where the head is rapidly decelerated upon contacting the stationary ground. This has been explained in terms of the CSF moving towards the impact site leaving the contrecoup site relatively deficient. This has been confirmed experimentally [21]. CSF has been seen to reduce the magnitude of the shear strains near the falx, the partition between the cerebral hemispheres, when the head is subject to rotational impact about the horizontal plane. Consequently, this implies that any computational model must consider the influence of the CSF when attempting to predict the physical response of the brain to a mechanical impact. The subarachnoid space, in which the CSF is contained, is non-existent over the surfaces of the gyri, is relatively small where the arachnoid bridges over small sulci and is much larger in certain locations where it bridges over large surface irregularities. Such regions, containing a considerable volume of CSF are called subarachnoid cisterns. Most analyses treat the CSF as a

layer of uniform depth [17, 22-24] whereas in reality it is a dispersed collection of discrete pockets along the longitudinal fissure.

Boundary conditions, such as the foramen magnum (the opening at the base of the skull), must also be considered carefully in any representative model. The presence of the foramen magnum allows the intracranial pressure to change during and subsequent to an impact. Representing the foramen magnum by a force free opening in combination with a no-slip interface [25] is likely to impose too strong a constraint on the movement of the brain through the opening for the spinal cord [26]. Sauren [26] suggested that using a slip condition at the skull-brain interface, together with a small opening around the spinal cord to represent the foramen, might provide a more realistic numerical solution. The kinematic neck boundary condition must also be modelled to allow the head respond realistically to impact. The most reasonable boundary condition probably depends on the impact condition (i.e., the distance from the head neck junction, regardless of whether the accelerations are translational or rotational) and these would allow some simplifying assumptions to be made in any model.

Mechanics and Mechanisms of Head Injury

A dynamic force applied to the head induces a complex series of mechanical and physical reactions involving local bending of the skull, volume changes to the intracranial contents, shock waves propagating throughout the brain and inertial effects, all of which induce tissue strains and stresses which may give rise to damage of the scalp, cranium, blood vessels or brain matter [18, 27]. It is clear that the mechanics that arise during a given head impact event are difficult to define [28]. This is not surprising as the consequence of the mechanics, i.e. tissue damage, seldom can be detected macroscopically and normally only can be observed by neurophysiological examination after the impact. The type of injury is determined by the location and severity of the mechanical distortion of the skull bone, blood vessels and brain tissue. These mechanical forces trigger a neurochemical cascade which involves the release of amino acid neurotransmitter molecules, the amount of which influence the extent of non-fatal lesions [29]. Rotational injuries may be produced by direct or indirect impacts to the head. Translational (linear) injuries involve direct linear acceleration of the head and lead to contusions while diffuse axonal injuries are commonly associated with rotational acceleration impacts. Concussion and haematomas may result from either translational or rotational acceleration impacts.

Shear strains that are induced within the brain as a result of the action of rotational accelerations can damage the bridging veins, thus leading to haemorrhaging (bleeding) and haematomas. As rotation continues over time, the shear strains would extend towards the inner area of the brain resulting in diffuse injuries. There is significant clinical evidence to support the belief that diffuse injuries are produced as a consequence of shearing of the brain tissues by rotational acceleration forces. However, the mechanics that govern rotational forces fails to explain the occurrence of coup and contrecoup injuries (i.e., at and opposite the site of impact, respectively) and it is currently accepted that translational (linear) acceleration is also responsible for causing severe injury.

After studying a number of post mortal cases and the blows that caused each death, Willinger et al. [30] deduced that impacts against hard surfaces lead to contusions and subdural haematomas, while impacts against soft surfaces give rise to diffuse axonal injury. An impact against a hard structure takes place over a shorter period while an impact with a soft structure results in a longer impact duration. A longer duration is required for the development of serious damage resulting from rotational acceleration than is required from translational acceleration. Hence, the dominant injuries for shorter impact durations are those that can be attributed to translation while those due to rotation are associated with longer impact durations. Soft structures act to absorb impact energy and decrease the conditions which cause focal injuries. However, they result in lower acceleration rates and the consequent longer duration of the impact pulses may aid the development of diffuse injuries.

Modelling Kinetics of Falls with Multibody Dynamics

A multibody system is a collection of rigid and flexible bodies joined together by kinematic joints (e.g., revolute or translational joints) and force elements (e.g., springs and dampers). It is possible to construct a multibody model of the human body with these kinematic joints and various discrete bodies of particular size and shape. The presence of these kinematic joints is conveniently accounted for in such a model by means of global and local coordinate reference systems (global would refer to the Cartesian coordinates of an initial reference frame while local would identify coordinates specific to an individual structural member such as the lower limb of a human). MADYMO (Mathematical Dynamic Models) [31] is a multibody dynamics simulation tool that has been developed to design and optimise automotive occupant safety systems, but which has a range of other related applications (accident reconstruction, injury biomechanics, vehicle handling, etc.). The multibody approach uses numerical algorithms to predict the motion of systems of bodies connected by kinematic joints, based on initial conditions and the inertial properties of the bodies.

A particular strength of this software is its database of human body models, including the family of multibody pedestrian models. They are available in five sizes: 50th percentile (average male), 95th percentile (large male), 5th percentile (small female), 6 year old child and 3 year old child. MADYMO's pedestrian model was originally adapted from the standing version of the Hybrid III crash test dummy, altering the joint stiffnesses of the lower extremities, neck and spine and contact characteristics of the pelvis, abdomen, ribs, shoulders and head in order to make it respond in a more realistically human manner. Head contact characteristics are based on the EEVC (European Experimental Vehicles Committee) adult headform model. The EEVC proposed in 1994 [32] a standard set of tests using various impactors that were designed to assess the potential risk to pedestrians from vehicle impacts. The MADYMO pedestrian models have a 'skeleton' consisting of chains of 52 bodies. The outer geometry of the pedestrian model is based on the RAMSIS software [33] and is represented using 64 ellipsoids (66 for the female). Deformation of soft tissue (flesh and skin) is represented by force-penetration characteristics assigned to each ellipsoid. These characteristics describe contact interactions of the pedestrian model with itself and with its environment.

Consider a typical falling accident, which resulted in focal head injury [34, 35]. An 11 year old boy (height 152cm, weight 37kg) suffering from heat exhaustion fainted after straightening up from drinking at a water fountain on a city street. Witnesses report that he fell straight backwards and that his head rebounded off the ground. The ground was reported to be level and concrete. Medical examination of this individual was carried out within 6 hours of injury, including head computed tomography (CT). A collateral history of the accident sequence was also taken from an eye-witness. The accident site was then examined in order to determine the layout of the environment, height of the fall, and the type of surface on which the person fell.

The patient experienced a brief loss of consciousness. Upon revival, his Glasgow Coma Scale (GCS) score was 14/15, indicating mild confusion. Detailed clinical examination of the patient revealed that the fall resulted in impact just over the occiput, mostly central, and slightly right-sided, as evidenced by subcutaneous bruising and swelling of the scalp overlying this region. There was no apparent skull fracture based on plain film and other radiological imaging and no other injuries were noted on full clinical trauma survey of this patient (i.e., neck, chest, abdomen, pelvis, and extremities). CT imaging on presentation to hospital revealed a right lateral frontal intracerebral haemorrhagic contusion, maximally measuring approximately 2 cm in the AP (anterior-posterior) plane x 3 cm in the ML (medial-lateral) plane x 6mm in the DV (dorso-ventral), beginning at the base of skull. There was also evident blood in the right Sylvian fissure seen on CT imaging (Fig. 2), representing a traumatic subarachnoid haemorrhage.

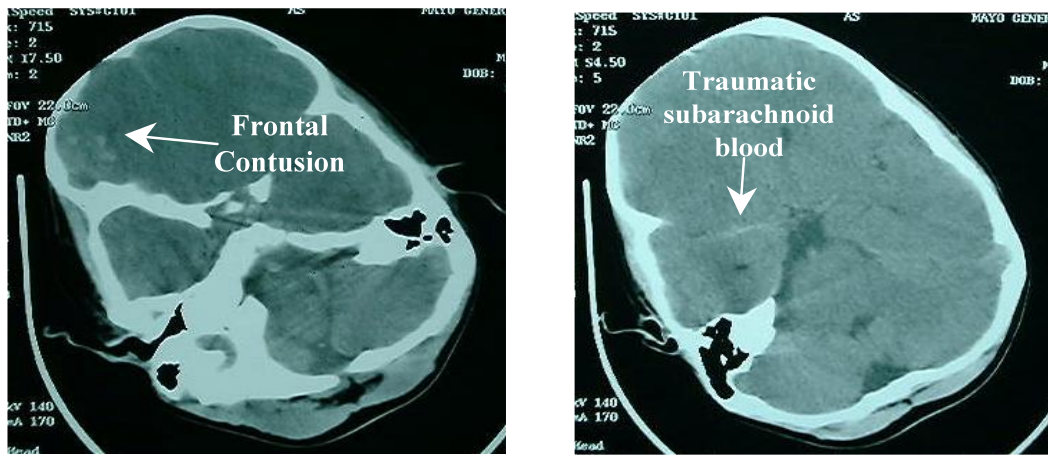


Figure 2. CT scans showing the intracranial injuries upon admission to hospital.

To model this case the 5th percentile female model was used (removing the ellipsoids representing the breasts). This model is designed to be 153cm in height and 49.8kg in weight. Thus the height of the model is quite accurate, but the weight is heavier than the boy. The only important feature in the environment is the pavement, which the head hit after fainting. This is modelled using a single plane in the inertial space, as seen in Fig. 3.

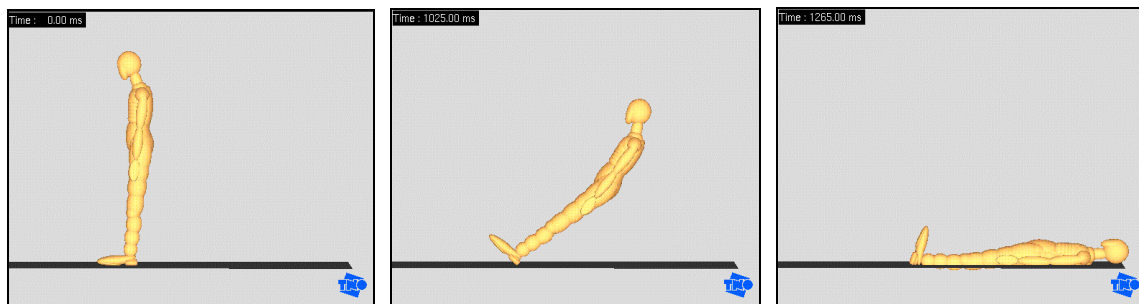


Figure 3(a) – (c). Sequence of motion during fainting fall.

For this simulation, the model was positioned on the plane leaning slightly backwards and allowed to fall freely with gravity: this was considered to correspond closest to the manner in which the boy fainted. It is unlikely in real life that this boy's legs would have remained fully straight when he fainted, as muscle activation is generally lost with loss of consciousness: this is a limitation on the accuracy of the simulation. Figures 3(a)-(c) show various time steps of the simulation. Peak results are shown in Table 1.

Table 1. Peak results for multibody dynamics simulation

Linear Velocity [m/s]	Angular Velocity [rad/s]	Linear Acceleration [g]	Angular Acceleration [rad/s ²]	Force [kN]
5.80	49.10	387	43,546	14.0

Coup and Contrecoup Contusion. The haemorrhagic contusion of the right frontal area is evidence of contrecoup injury, with no coup contusion evident. This is in line with general findings on brain injury due to falls. The linear acceleration can be compared to the lower tolerance curve for contusion proposed by Auer et al. [36]. This is suggested as the minimum linear acceleration required for contusion to occur. For the present case, linear acceleration levels exceed this lower tolerance limit: this suggests that the presence of contusion is likely. And, indeed, contusion is present in this case. However, it must be noted that rotation is also thought to play a part in causing contusion. Angular velocity is quite high in this case and angular acceleration extremely high.

However, no tolerance curves exist within the literature relating angular motion to contusion against which to compare the results found here.

Skull Fracture. As can be seen in Table 1, the predicted peak force was 14.0 kN. This is slightly greater than the force measured by Yoganandan *et al.* [37] as being necessary to fracture cranial bone. It is within the range of force values found by Allsop *et al.* [38] for skull fracture. Clinically, there was no skull fracture in this case. However, when the age of this person is considered, the average skull stiffness of an 11 year old boy is less than that of an adult. The skull does not become fully calcified until adulthood, and Mohan *et al.* [39] suggest that at age 13, skull stiffness is approximately 90% of that of an adult. Hence, at the age of 11, it is likely that the skull of this boy is more compliant than that of an adult. If an appropriately lower rigidity were taken into account in the force-penetration curves for head contact, the resultant forces on the head would be predicted to be lower. These, in turn, would reduce the predicted linear and angular accelerations, and would thus affect the relationship of predicted results to established tolerance curves for various forms of head injury.

Subarachnoid Haemorrhage. Auer *et al.* [36] found a good relationship between linear acceleration and the occurrence of subarachnoid haematoma. The predicted peak linear acceleration exceeds the lower tolerance limit and falls just below the upper tolerance limit suggested by Auer for the occurrence of subarachnoid haematoma. This agrees with the observed injuries in this case, where there was indeed subarachnoidal haemorrhaging.

Cerebral Concussion/Diffuse Brain Injury. The predicted angular acceleration is very high in this case, but the corresponding angular velocities are not so high. Compared to the 5% and 10% critical strain curves proposed by Margulies and Thibault [40], the combination of angular velocity and acceleration is close to the 5% strain curve, suggesting that DAI could occur. Below the 10% curve it is likely that less severe diffuse injury might occur, such as cerebral concussion. There is mild concussion in this case. Indeed there is loss of consciousness, which is indicative of more than merely 'mild' concussion. However, it is unknown in this case whether the loss of consciousness can be attributed partly to the head injury, or whether it was only due to the boy fainting. Linear acceleration values exceed the tolerance curve proposed by Ono *et al.* [41] for concussion in humans.

Finite Element Model of Human Head

The geometry of a male and a female human cadaver has been determined by Computed Tomography (CT), Magnetic Resonance Tomography (MRT) and sliced colour photographs. The geometric data are available through the Visible Human Database (National Institute of Health, USA) with 0.3 mm incrementation in the coronal plane [42]. A three-dimensional finite element (3DFE) model was created using this CT data [43]. Such digitised data is made up of voxels, which can be considered to be three-dimensional pixels. The scans are stored in stacks which make a stepped volume sampled recording. Interpolation and thresholding schemes were used to identify voxels representing bone, for example, and interpolate through the voxel generating smooth triangulated surfaces closer to the shape of the actual scanned head. The CT data was used to create a polygonal model of the visible male skull using vtk-software [44]. The resulting polygonal model was decimated and smoothed in order to make the model more portable. This then was converted into IGES format and imported into the commercially available software MSC/Patran [45].

The 3DFE model of the skull-brain complex includes scalp, a 3-layered skull (outer and inner tables, diploe), dura, CSF, pia, falx, tentorium, cerebral hemispheres, cerebellum and brain stem. This is shown in cutaway view in Fig. 4. Meshing was an issue that arose in previous models [17, 23, 24, 46-48] but in the present model much emphasis was placed on mesh quality and ease of mesh creation, without sacrificing anatomical accuracy. For example, the ridge of the sphenoid wing, or the cusp of the skull upon which the temporal lobe sits, does not have an element face

traversing it, which would necessitate a smoothing of this ridge (for element quality), but still avoids problems which have been associated with other models [46].

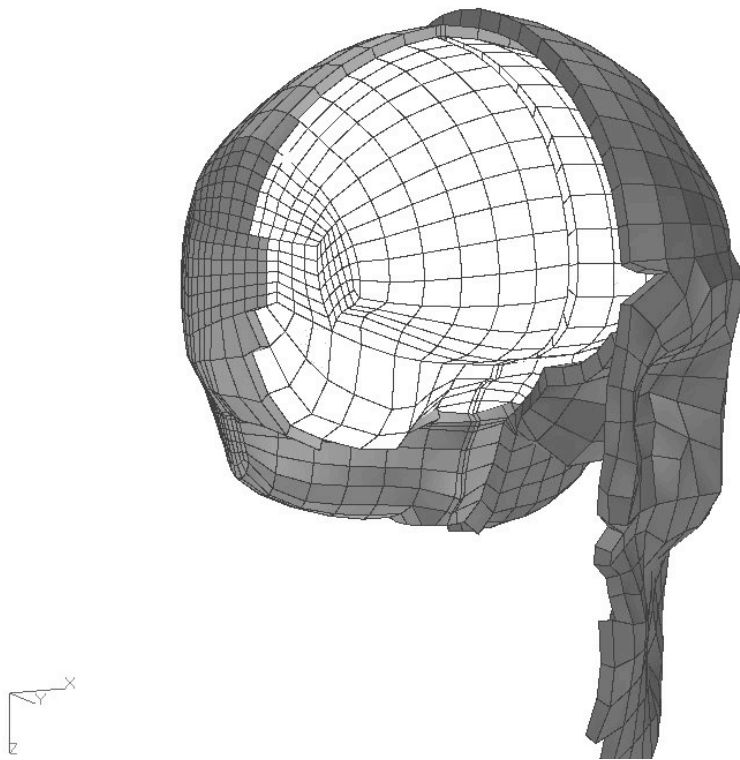


Figure 4. Medium density mesh with 1.3mm thick CSF layer. Dark shading represents facial bone. A section cutaway of the 3-layered skull is visible, underneath which is shown a small amount of CSF (shaded in grey). The brain elements are shown in white.

Constitutive Properties

The constitutive properties of human brain have been the subject of much research within recent decades. Since these properties cannot be obtained by means of in vivo tests on humans, alternative methods have been used such as in vivo tests on primates with an associated scaling law or an in vitro examination of human brains. The main concern with the former method is the lack of an adequate scaling law [49], whilst it is uncertain how the properties obtained from the latter method are altered as the brain dries out once blood supply has ceased [10].

The tissues of the brain are quite heterogeneous on both the macroscale and the microscale. The mechanical properties of the brain and CSF will affect the pressure response of the brain. Thus any model of the intracranial system that is excessively stiff or compliant will not accurately simulate a physical head response. The intracranial contents have, on the whole, been treated as incompressible comparable with water. However, the brain tissues are more similar to a gel-like material containing approximately 77-78% water. The opening at the base of the skull, the foramen magnum, and the presence of the lateral ventricles allow the pressure of the intracranial contents to change. The fact that the ventricles are filled with CSF and many blood vessels are present in the brain indicates that the bulk modulus of the brain should be somewhat lower than that of water. Since brain motion can lag behind that of the skull during an impact the fluid in the subarachnoid space would be expected to have a lower shear modulus and bulk modulus than that of the brain in order to represent the fact that it can move within the skull.

Identifying correct constitutive properties for neural tissue continues to be a limiting restriction in computational modelling. Earlier finite element models of the brain adopted linear elastic material constitutive laws [47, 48, 50]. In recent studies, linear viscoelastic material laws combined with large-deformation theory were used to model brain tissues [17, 51, 52], except for the work of

Mendis [53], who employed nonlinear viscoelastic materials under large-deformation. It is generally believed that brain tissue is a highly damped material. Thus, a linearly viscoelastic material model combined with a large-deformation theory was chosen to model brain tissue in the present author's investigations. The behaviour of this material was characterised as viscoelastic in shear with a deviatoric stress rate dependent on the shear relaxation modulus, while the compressive behaviour of the brain was considered as elastic. The shear characteristics of the viscoelastic behaviour of the brain was expressed by:

$$G(t) = G_{\infty} + (G_0 - G_{\infty})e^{-\beta t}. \quad (1)$$

G_{∞} is the long term shear modulus, G_0 is the short term shear modulus and β is a decay factor.

The CSF layer was modelled using solid elements with a low shear modulus as has been done by others [17, 19, 20, 24, 54, 55]. Due to computational constraints, it was not feasible to model a sliding boundary condition between the interfaces of the skull/CSF/brain. The depth of the CSF layer was chosen to be either 1.3mm or 3mm, the former corresponding more closely to an adult and the latter to a very elderly person. The bulk modulus for the fluid was very high and as such use was made of the hybrid elements in ABAQUS [56]. Near-incompressible behaviour occurs when the bulk modulus is very much larger than the shear modulus (usually where the Poisson's ratio is greater than 0.48) and exhibits behaviour approaching the incompressible limit: a very small change in displacement produces extremely large changes in pressure. Therefore, a purely displacement based solution is too sensitive to be useful numerically. This singular behaviour is removed from the calculations in ABAQUS by treating the pressure as an independently interpolated basic solution variable, coupled to the displacement solution through the constitutive theory and the compatibility condition. This independent interpolation of pressure is the basis of the hybrid element.

The material properties for the remaining parts of the model, i.e., the cortical and trabecular bone, scalp and intracranial membranes were taken from the literature [17, 22, 24, 57]. Table 2 summarises the mechanical properties that were used in the subsequent analyses. The weight of the model when scaled to the dimensions of the cadaver skull of experiment 37 of Nahum [58] was 4.017kg whilst the brain weighed 1.422kg. The inertial properties are $I_{YY} = 1795 \text{ kg.mm}^2$, $I_{ZZ} = 1572 \text{ kg.mm}^2$ and $I_{XX} = 1315 \text{ kg.mm}^2$, similar to those of [22].

Table 2. Constitutive properties used in 3DFE head model

Material	Young's Modulus [MPa]	Poisson's ratio	Density [kg/m ³]
Scalp	16.7	0.42	1000
Cortical Bone	15000	0.22	2000
Trabecular Bone	1000	0.24	1300
Dura	31.5	0.45	1130
Pia	11.5	0.45	1130
Falx and Tentorium	31.5	0.45	1130
Brain	Hyperelastic	0.499981	1040
Facial Bone	5000	0.23	2100

To illustrate the use of this 3DFE head model, an instrumented cadaveric head impact experiment [58] was simulated. The predicted pressure-time histories were compared directly against those obtained experimentally. The analysis was undertaken using ABAQUS 5.8 [56].

The model was oriented in the same manner as Nahum's original experiment. The head was rotated forward at 45° to the frankfort plane. A frontal impulse was applied in the sagittal plane in an anterior to posterior direction. The load form was approximately a semi-sinusoidal pulse of peak magnitude 7000N and duration 6ms. Since the neck restraint is unlikely to affect the head response in a short duration (< 6ms) impact [17], a free boundary condition was assumed in the analysis.

The particular model that was used for this simulation was a medium meshed model with a thin CSF depth. It was warped to the dimensions of the cadaver head of experiment 37 of [58]. It used the same material properties of [53], which were also used by [22]. A hyperelastic material was used for the brain to maintain these properties, in conjunction with a viscoelastic material property, giving the material a decay factor of $\beta = 145\text{s}^{-1}$. The hyperelastic law was given by:

$$C_{10}(t) = 0.9C_{01}(t) = 620.5 + 1930e^{(-t/0.008)} + 1103e^{(-t/0.15)}. \quad (2)$$

C_{10} and C_{01} are temperature-dependent material parameters with units of Pa, and time t is in seconds.

The experimental results obtained by Nahum are not full-field data, unlike those of the present FE simulations. Rather, they are discrete point-wise results that were obtained from transducers located at particular regions of the head. In order to compare the present simulations with the experimental results, four specific locations were selected from the FE model, namely (i) the frontal coup site, adjacent to the impact site, (ii) the parietal site, (iii) the occipital site and (iv) the contrecoup site, opposite the impact site. Figure 5 shows the correlation of the simulated and experimental pressure time histories for the impact.

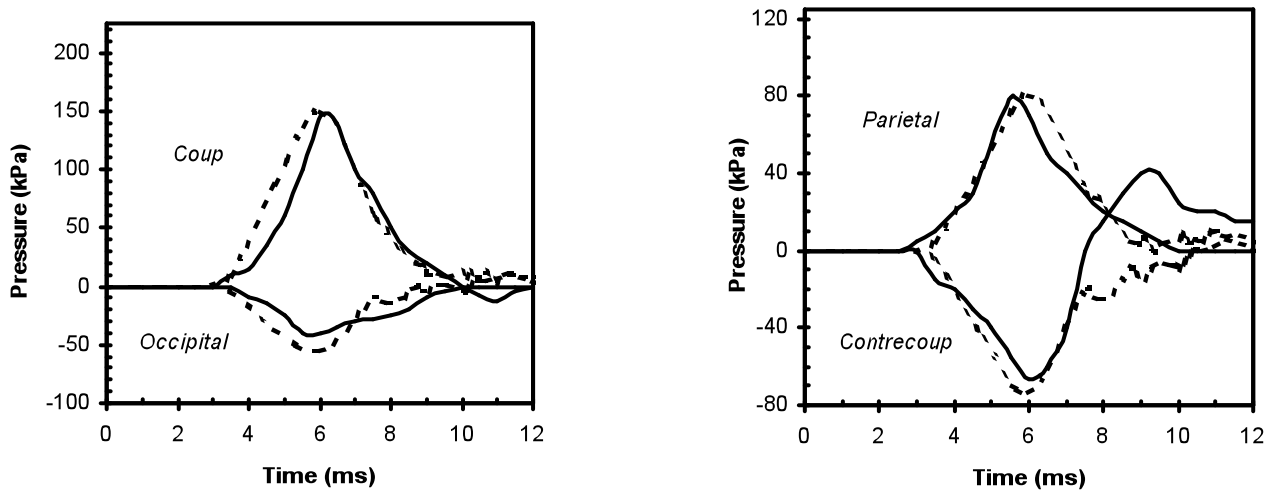


Figure 5. Comparison between intracranial pressures measured experimentally [58] (solid lines) and predicted by 3DFE simulation (dashed lines)

The correlation is good and as such the model can be considered to predict the physical response of the impact well. The maximum pressures that are numerically predicted to develop within the four distinct regions of the brain, the specific shape of the various pressure-time response curves and the particular duration of pressure pulses are all in close agreement with those that were measured experimentally by Nahum et al. [58].

Conclusions

This paper reports on the status of ongoing research efforts to simulate the effects of accidental head impacts using two separate computational techniques. The first, multibody dynamics simulations, can model the kinematics and resulting force distributions that a body would sustain during a fall. The second, three-dimensional finite element analyses, requires knowledge of the predicted force-time history in order to estimate the full-field distribution of stress and strain within the cranium. A comparison of predicted results against various injury criteria can indicate the likely severity of associated trauma.

Whilst these two computational mechanics techniques have not yet been integrated, it is evident that this methodology offers potential for simulating *real life* accident events and predicting the resulting neurotrauma. Such a procedure could be used to customize surgical interventions for particular patients or to develop optimised safety equipment for specific groups of people.

Acknowledgements

This research has been undertaken by various research students in the author's laboratory in University College Dublin: D. O'Donoghue, J.D. Finan, T. Horgan and K. O'Riordain and has involved collaboration with Prof. J.P. Phillips and Dr P.M. Thomas of the National Department of Neurosurgery, Beaumont Hospital, Dublin. The generous financial support that has been provided by Enterprise Ireland (SC/99/237), University College Dublin (President's Research Award) and the PRTL programme of the Higher Education Authority (National Neuroscience Network and UCD's Conway Neuroscience) is gratefully acknowledged.

References

- [1] Jennett, B., 1996, Epidemiology of head injury. *Journal of Neurology, Neurosurgery & Psychiatry*, **60**, pp. 362-369.
- [2] Ommaya, A.K., Thibault, L. & Bandak, F.A., 1994, Mechanisms of impact head injury. *International Journal of Impact Engineering*, **15**, pp. 535-560.
- [3] Mortensen, K., Romner, B. & Ingebrigsten, T., 1999, Epidemiology of head injuries in Troms. *Tidsskr Nor Laegeforen*, **119**, pp. 1870-1873.
- [4] Meerhoff, S.R., de Kruijk, J.R., Rutten, J., Leffers, P. & Twijstra, A., 2000, Incidence of traumatic head or brain injuries in catchment area of Academic Hospital Maastricht in 1997, *Ned Tijdschr Geneesk*, **144**, pp. 1915-1918.
- [5] Vazquez-Barquero, A., Vazquez-Barquero, J.L., Austin, O., Pascual, J., Gaité, L. & Herrera, S., 1992, The epidemiology of head injury in Cantabria, *European Journal of Epidemiology*, **8**, pp. 832-837.
- [6] Watson, W.L. & Ozanne-Smith, J., 2000, Injury surveillance in Victoria, Australia: Developing comprehensive injury incidence estimates, *Accident Analysis and Prevention*, **32**, pp. 277-286.
- [7] Scallan, E., Staines, A., Fitzpatrick, P., Laffoy, M. & Kelly, A., 2001, Injury in Ireland, Report of the Department of Public Health Medicine and Epidemiology, University College Dublin.
- [8] Yanagida, Y., Fugiwara, S. & Mizoi, Y., 1989, Differences in intracranial pressure caused by a 'blow' and/or a 'fall' – An experimental study using physical models of the head and neck, *Forensic Science International*, **41**, pp. 135-145.
- [9] Manavais, J., Blumbergs, P.C., Scott, G. & North, J.B., 1991, Brain injury patterns in falls causing death. *Proceedings of the International IRCOBI Conference on the Biomechanics of Impact*, pp. 77-88.
- [10] Viano, D.C., King, A., Melvin, J.W. & Weber, K., 1989, Injury biomechanics research: an essential element in the prevention of trauma, *ASME Journal of Biomechanical Engineering*, **22**, pp. 403-417.
- [11] Dassios, G., Kiriakopoulos, M. K. & Kostopoulos, V., 1998, On the sensitivity of the vibrational response of the human head, *Computational Mechanics*, **21**, 382-388.

-
- [12] Nisitani, H. & Chen, D. H., 1997, Body force method and its application to numerical and theoretical problems in fracture and damage, *Computational Mechanics*, **19**, 470-480.
- [13] Holbourn, A. H. S., 1943, Mechanics of head injury, *Lancet*, **2**, pp. 438-441.
- [14] Goldsmith, W., 1972, *Biomechanics of Head Injury: Biomechanics, Its Foundations and Objectives*. Prentice-Hall.
- [15] Gurdjian, E. S., 1972, Recent advances in the study of the mechanism of impact injury of the head – A summary, *Clinical Neurosurgery*, **18**, pp. 1-42.
- [16] Misra, J. C. & Chakravarty, S., 1983, A study on rotational brain injury, *ASME Journal of Biomechanical Engineering*, **17**, pp. 459-466.
- [17] Ruan, J. S., 1994, *Impact Biomechanics of Head Injury by Mathematical Modelling*, PhD thesis, Wayne State University.
- [18] O'Donoghue, D., 1999, *Biomechanics of Frontal and Occipital Head Impact Injuries: A Plane Strain Simulation of Coup and Contrecoup Contusion*, MEngSc thesis, University College Dublin.
- [19] Gilchrist, M. D. & O'Donoghue, D., 2000, Simulation of the development of frontal head impact injury, *Computational Mechanics*, **26**, pp. 229-235.
- [20] Gilchrist, M. D., O'Donoghue, D. & Horgan, T. J., 2001, A two-dimensional analysis of the biomechanics of frontal and occipital head impact injuries, *International Journal of Crashworthiness*, **6**, pp. 253-262.
- [21] Edberg, S., Rieker, J. & Angrist, A., 1963, Study of impact pressure and acceleration in plastic skull models, *Labs. Invest.*, **12**, pp. 1305-1311.
- [22] Kleiven, S. & Von Holst, H., 2002, Consequences of size following trauma to the human head, *Journal of Biomechanics*, **35** pp. 135-160.
- [23] Willinger, R., Kopp, C. M. & Cesari, D., 1992, New concept of contrecoup lesions: Modal analysis of a finite element head model, *Proceedings of the International IRCOBI Conference on the Biomechanics of Impacts*, pp. 283-298.
- [24] Zhou, C., Khalil, T. B. & King, A., 1996, Viscoelastic response of the human brain to sagittal and lateral rotational acceleration by finite element analysis, *Proceedings of the International IRCOBI Conference on the Biomechanics of Impacts*, pp. 35-48.
- [25] Lee, E. S., 1990, *A Large-Strain, Transient-Dynamic Analysis of Head Injury Problems by the Finite Element Method*, PhD thesis, Georgia Institute of Technology.
- [26] Sauren, A. A. H. J. & Claessens, M. H. A., 1993, Finite element modeling of head impact: The second decade, *Proceedings of the International IRCOBI Conference on the Biomechanics of Impacts*, pp. 241-251.
- [27] O'Donoghue, D. & Gilchrist, M. D., 1998, Strategies for modelling brain impact injuries, *Irish Journal of Medical Science*, **167**, pp. 263-264.
- [28] Jones, S. E., Rule, W. K., Jerome, D. M. & Klug, R. T., 1998, On the optimal nose geometry for a rigid penetrator, *Computational Mechanics*, **22**, pp. 413-417.
- [29] Smyth, A., Gallagher, C. Gilchrist, M. D. & O'Connor, W. T., 2002, Animal models of traumatic brain injury: A critical evaluation. Paper 15, *Proceedings of the Irish Neuroscience Group Annual Meeting*.
- [30] Willinger, R., Ryan, G. A., McLean, A. J. & Kopp, C. M., 1992, Mechanisms of brain injury related to mathematical modeling and epidemiological data, *Proceedings of the International IRCOBI Conference on the Biomechanics of Impacts*, pp. 179-192.
- [31] TNO Automotive, 1999, MADYMO, Version 5.4.1. The Hague, NL.
- [32] EEVC Working Group 10 Report, 1994, Proposals for methods to evaluate pedestrian protection for passenger cars.
- [33] Speyer, H. & Seidl, A., 1997, RAMSIS – A new CAD tool for ergonomic analysis of vehicles developed for the German automotive industry. *SAE Paper Number 970088*.
- [34] O'Riordain, K., 2002, *Reconstruction of Real World Head Injury Accidents Resulting from Falls Using Multibody Dynamics Modelling*, MEngSc thesis, University College Dublin.

-
- [35] O’Riordain, K., Thomas, P. M., Phillips, J. P. & Gilchrist, M. D., 2003, Reconstruction of real world head injury accidents resulting from falls using multibody dynamics modelling, *Clinical Biomechanics*, in press.
- [36] Auer, C., Schonpflug, M. Beier, G. & Eisenmenger, W., 2001, An analysis of brain injuries in real world pedestrian accidents by computer simulation reconstruction, *Proceedings of International Society of Biomechanics XVIIIth Congress*.
- [37] Yoganandan, N., Pintar, F.A., Sances Jr., A., Walsh, P.R., Ewing, C.L., Thomas, D.J. & Snyder, R.G., 1995, Biomechanics of skull fractures. *Journal of Neurotrauma*, **12**, pp. 659-668.
- [38] Allsop, D.L., Perl, T.R. & Warner, C.Y., 1991, Force/deflection and fracture characteristics of the temporo-parietal region of the human head, *Proceedings of the 35th Stapp Car Crash Conference*, Society of Automotive Engineers, pp. 269-278.
- [39] Mohan, D., Bowman, B.M., Snyder, R.G. & Foust, D.R., 1979, A biomechanical analysis of head impact injuries to children, *ASME Journal of Biomechanical Engineering*, **101** pp. 250-260.
- [40] Margulies, S.S. & Thibault, L.E., 1992, A proposed tolerance criterion for diffuse axonal injury in man, *Journal of Biomechanics*, **25**, pp. 917-923.
- [41] Ono, K., Kikuchi, A., Nakamura, M. & Kobayashi, H., 1980, Human head tolerance to sagittal impact reliable estimation deduced from experimental head injury using subhuman primates and human cadaver skulls, *Proceedings of 24th Stapp Car Crash Conference*, Society of Automotive Engineers, pp. 101-160.
- [42] National Institutes of Health (NIH) U.S. National Library of Medicine, Department of Health and Human Services, Visible Human Database, <www.nlm.nih.gov/research/visible/visible_human.html>.
- [43] Horgan, T. J. & Gilchrist, M. D., 2003, The creation of three-dimensional finite element models for simulating head impact biomechanics, *International Journal of Crashworthiness*, in press.
- [44] Lorensen, B., VTK open source software, <<http://public.kitware.com/VTK/>>.
- [45] Patran r2a, 2002, MSC/Patran User’s Manual, MSC.
- [46] Claessens, M., Sauren, A. A. H. J. & Wismans, J. S. H. M., 1997, Modelling of the human head under impact conditions: A parametric study, *Proceedings of 41st Stapp Car Crash Conference*, SAE Paper Number 973338, Society of Automotive Engineers, pp. 315-328.
- [47] Shugar, T. A. & Katona, M. G., 1975, Development of a finite element head injury model, *ASCE Journal of Engineering Mechanics*, **173**, pp. 223-239.
- [48] Ward, C. & Thompson, R., 1975, The development of a detailed finite element brain model, *Proceedings of 19th Stapp Car Crash Conference*, SAE Paper Number 751163, Society of Automotive Engineers.
- [49] Ljung, C., 1978, *On Scaling in Head Injury Research*, Lund Institute of Technology.
- [50] Hosey, R. R. & Liu, Y. K., 1982, Finite elements in biomechanics, in *A Homeomorphic Finite Element Model of the Human Head and Neck*, BR Johnson, TC Gallagher, RH Simon & JF Gross (Eds), pp. 379-401, Wiley.
- [51] DiMasi, F., Marcus, J. H. & Eppinger, R. H., 1991, 3-D anatomic brain for relating cortical strains to automobile crash loading, *Proceedings of 13th International Technical Conference on Experimental Safety Vehicles*, Paper Number 91-S8-O-11.
- [52] Turquier, F., Kang, H. S., Trosseille, Willinger, R., Lavaste, F., Tarriere, C. & Domont, A., 1996, Validation study of a 3D finite element head model against experimental data, *Proceedings of 40th Stapp Car Crash Conference*, SAE Paper Number 962431, Society of Automotive Engineers.
- [53] Mendis, K. K., Stalnaker, R. L. & Advani, S. H., 1995, A constitutive relationship for large deformation finite element modeling of brain tissue, *ASME Journal of Biomechanical Engineering*, **117**, pp. 279-285.

-
- [54] Kang, H., Willinger, & Diaw, B. M., 1997, Validation of a 3D anatomic human head model and replication of head impact in motorcycle accident by finite element modeling, *Proceedings of 41st Stapp Car Crash Conference*, Society of Automotive Engineers, pp. 329-328.
- [55] Hao Hu, Nayfeh, A. H. & Rosenberg, W. S., 1998, Modeling of human brain movability during impact, *Proceedings 5th International LS DYNA Users Conference*.
- [56] ABAQUS 5.8, 2000, *ABAQUS/Standard User's Manual*, HKS.
- [57] Willinger, R., Taleb, L. & Kopp, C. M., 1995, Modal and temporal analysis of head mathematical models, *Journal of Neurotrauma*, **12**, pp. 743-754.
- [58] Nahum, A. M., Smith, R. W. & Ward, C. C., 1977, Intracranial pressure dynamics during head impact, *Proceedings of 21st Stapp Car Crash Conference*, *SAE Paper Number 77-922*, Society of Automotive Engineers.